Physics Letters B 278 (1992) 187–192
North-Holland

PHYSICS LETTERS B

Higgs boson production in eγ collisions

K. Hagiwara [a,b], I. Watanabe [c] and P.M. Zerwas [d]

[a] *Department of Physics, University of Durham, Durham DH1 3LE, UK*
[b] *Theory Group, KEK, Tsukuba, Ibaraki 305, Japan*
[c] *Department of Physics, Hiroshima University, Higashi-Hiroshima 724, Japan*
[d] *Deutsches Elektronen-Synchrotron, DESY, W-2000 Hamburg 52, FRG*

Received 3 December 1991

A large number of W bosons can be produced in high energy e^+e^- linear colliders through the subprocess $\gamma+e\to W+\nu$, with the photons generated by back-scattering of laser light. We have explored to which extent this process can be exploited to produce Higgs bosons through emission from the W line: $\gamma+e\to W+H+\nu$. For very high energies, photoproduction of Higgs bosons on a W-boson target, $\gamma+W\to W+H$, is the dominant fundamental subprocess.

It is well known that a large number of single W bosons can be produced in high energy e^+e^- linear colliders [1]. The main production mechanism is provided by the process $\gamma+e\to W+\nu$. The photon flux is generated automatically by Weizsäcker–Williams photons and by beamstrahlung in the collision of high-density e^- and e^+ bunches. However, a large flux of photons, with an average energy only slightly reduced in comparison with the e-beam energy, can be generated by Compton back-scattering of laser light [2].

The large cross section for W production suggests that this process can be exploited as a source for Higgs bosons emitted from the W-boson line, fig. 1,

$$\gamma+e\to W+H+\nu\,. \tag{1}$$

In an exploratory study we have determined the cross section for this reaction. The rates have been evaluated for two extreme cases by choosing the flux of high energy photons generated by Compton back-scattering of laser light and, on the other hand, the Weizsäcker–Williams spectrum for quasi-real photons. Since the final state consists of three particles, two of which are heavy, the cross section at moderate energies ($\sqrt{s}\sim 500$ GeV) is smaller than the cross section for the standard W fusion mechanism $e^+e^-\to\bar{\nu}\nu H$ and the bremsstrahlung process $e^+e^-\to ZH$. However, at high energies ($\sqrt{s}\gtrsim 1$ TeV) the cross section for the process (1) is similarly large as that of the dominant $\bar{\nu}\nu H$ process for most of the m_H range accessible at linear colliders, and significantly larger than the cross section of the bremsstrahlung process. A dedicated eγ collider with back-scattered laser beam

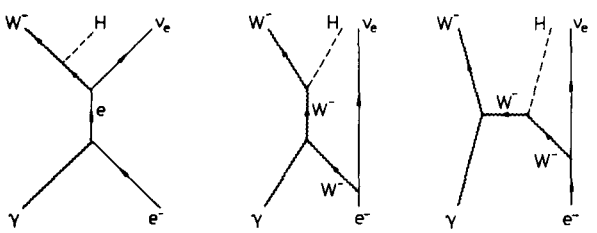

Fig. 1. Feynman diagrams for the process $\gamma+e^-\to W^-+H+\nu_e$. The two last diagrams build up the subprocess $\gamma+W^-\to W^-+H$, photoproduction of Higgs particles on a W-boson target.

therefore gives rise to a large Higgs production cross section through the process (1), providing us, for instance, with the opportunity to study the WWH coupling in the W+H channel.

At high energies, the basic subprocess reduces to the reaction

$$\gamma + W \to W + H , \tag{2}$$

i.e. the photoproduction of Higgs particles on W-boson targets, one of the fundamental processes in the electroweak sector. We present the complete analytic expressions for the helicity amplitudes of this reaction. For sufficiently heavy Higgs bosons ($m_H^2 \gg m_W^2$), the subprocess (2) reduces further to the standard $W_L W_L$ fusion production ($W_L^+ W_L^- \to H$) where one of the two effectively real longitudinal W bosons (W_L) is created by the splitting of the real photon. We present the effective W_L distribution inside a photon, that describes well the asymptotic behavior of the cross section.

We have calculated the cross section (1) by utilizing the HELAS program [1,3,4], in which the helicity amplitudes are generated at the tree level (fig. 1). By introducing the five external wavefunctions, the initial photon (A) and electron ($|e\rangle$) and the final W boson (W). Higgs boson (H) and neutrino ($\langle\nu|$), the Feynman amplitudes of fig. 1 are expressed as

$$\mathcal{M} = \langle\nu|J_W(W,H)|e,A,e\rangle + \Gamma_{WW3}(J_W(W,H), J_W(\langle\nu|, |e\rangle), A) + \Gamma_{WWH}(J_W(W,A), J_W(\langle\nu|, |e\rangle), H) , \tag{3}$$

where each term corresponds to each of the three diagrams. For instance, $J_W(W, H)$ represents the off-shell W wave-function built-up by the external lines W and H: $|e, A, e\rangle$ represents the off-shell electron wave-function made of the external lines A and $|e\rangle$. The first diagram is expressed as a vertex of the off-shell W, the off-shell electron and the external neutrino, the second one is a vertex of two off-shell W's and the photon, and the last diagram is a vertex of two off-shell W's and H. The external wave-functions, the off-shell lines and the vertices are then calculated numerically by the HELAS subroutines [1,3,4].

The results for the cross sections are shown in fig. 2 for fixed $e\gamma$ CM energies between 200 and 2000 GeV, and Higgs masses varying from 50 to 500 GeV. It is obvious that for moderate Higgs masses and high CM energies the magnitude of the cross sections is large enough for the process to become interesting experimentally.

These cross sections must be averaged over the photon flux. Since the spectrum of beamstrahlung photons depends strongly on the machine design, we have restricted our discussion to the standard soft Weizsäcker–Williams spectrum and, on the other hand, to the hard γ spectrum generated by Compton back-scattering of laser light. The results for beamstrahlung photons are expected to fall between these two extreme cases. Since we present the Weizsäcker–Williams photons just for comparison, we have adopted the simplest EPA form of the spectrum

$$D_{\gamma/e}^{EPA}(z) = \frac{\alpha}{2\pi}\left(\log\frac{s}{m_e^2} - 1\right)\frac{1-(1-z)^2}{z} , \tag{4}$$

where $z \leqslant 1$ denotes the fraction of energy transferred from the electron/positron to the photon. The spectrum is soft and falls sharply with increasing γ energy. By contrast, the spectrum of the back-scattered laser photons is hard [2].

$$D_{\gamma/e}^{LASER}(z) = \frac{2(1+y)^2}{(1-z)^2}\,\frac{2y^2 - 4y(1+y)z + (4+4y+3y^2)z^2 - y^2z^3}{y(16+32y+18y^2+y^3) - 2(8+20y+15y^2+2y^3-y^4)\log(1+y)} . \tag{5}$$

The parameter y depends on the laser-photon frequency ω, $y = 2\sqrt{s}\omega/m_e^2$; for $\omega = 1.26$ eV [5] the value is given by $y = 4.8$ at $\sqrt{s} = 500$ GeV and larger still for higher energies. However, due to the onset of e^+e^- pair production between laser photons and back-scattered photons at $y > 2 + 2\sqrt{2} \approx 4.82$ [2,5], the conversion efficiency drops

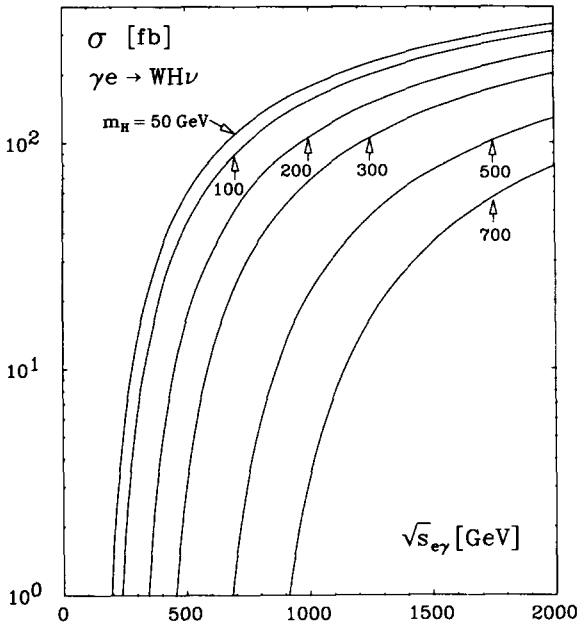

Fig. 2. Total cross section of the process $\gamma+e^-\to W^-+H+\nu_e$ versus the $e\gamma$ CM energy for several values of the Higgs mass m_H.

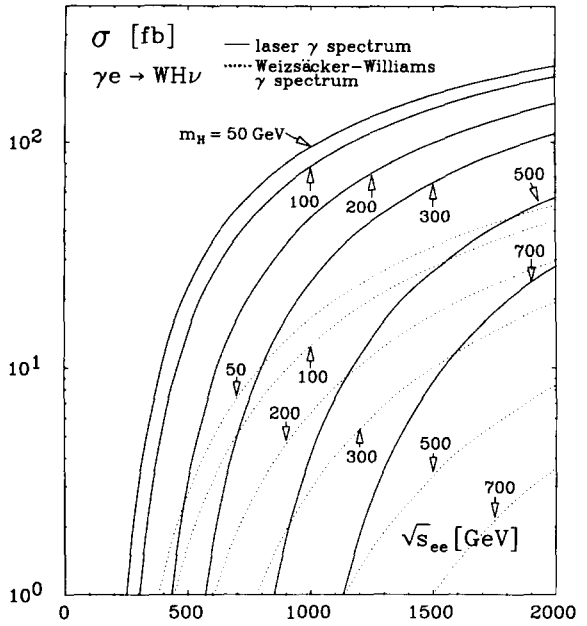

Fig. 3. Total cross section of the process $\gamma+e^-\to W^-+H+\nu_e$ averaged over the photon flux generated by Compton back-scattering of laser light (full lines). $\sqrt{s}$ is the total e^+e^- CM energy. The dotted lines represent the cross section folded with the Weizsäcker–Williams photon spectrum.

considerably beyond this threshold value. Therefore we shall assume $y=4.82$ in the subsequent discussion [#1]. The spectrum [#2] peaks at the maximum z value that can be realized kinematically, $z_{max}=y/(1+y)=0.83$. The experimental cross sections are then evaluated by folding $\sigma(\gamma e\to WH\nu)$ with the spectra (4) and (5),

$$\langle\sigma(\gamma e\to WH\nu)\rangle=\int_{z_{min}}^{z_{max}} dz\, D_{\gamma/e}(z)\sigma(\gamma e\to WH\nu;\hat{s}=zs)\,. \tag{6}$$

This formula applies for a single W charge; in the Weizsäcker–Williams case the cross section is doubled by adding up the W^+ and W^- channels.

The full curves in fig. 3 present the results after folding the basic cross sections with the spectrum for back-scattered laser photons. The final cross sections for the Weizsäcker–Williams spectrum are indicated by the dotted lines. It follows that laser induced $e\gamma$ collisions even at 500 GeV e^+e^- CM energy provide significantly large WH production rates. With an integrated luminosity of $\int\mathscr{L}=10$ fb^{-1}, of the order of 200 events are produced for a Higgs mass of about 100 GeV. The cross section grows rapidly with the colliding e^+e^- energy, and at a 1 TeV collider we can expect more than 100 events for the same integrated luminosity up to a Higgs mass of 500 GeV. The cross sections for the Weizsäcker–Williams equivalent photon flux (dotted lines) is significantly smaller at all energies, and they are of practical interest only at energies beyond 1 TeV for light Higgs boson.

In fig. 4 we show the Higgs photoproduction cross section for the two extreme photon spectra (solid lines for

[#1] For machine designs with high repetition rate and low luminosity per bunch crossing, the underlying $\gamma\gamma$ induced hadronic backgrounds are negligibly small. We thank M. Drees for a discussion about this problem.

[#2] For a plot of the spectrum, see e.g. fig. 22 of ref. [6] or fig. 2 of ref. [7].

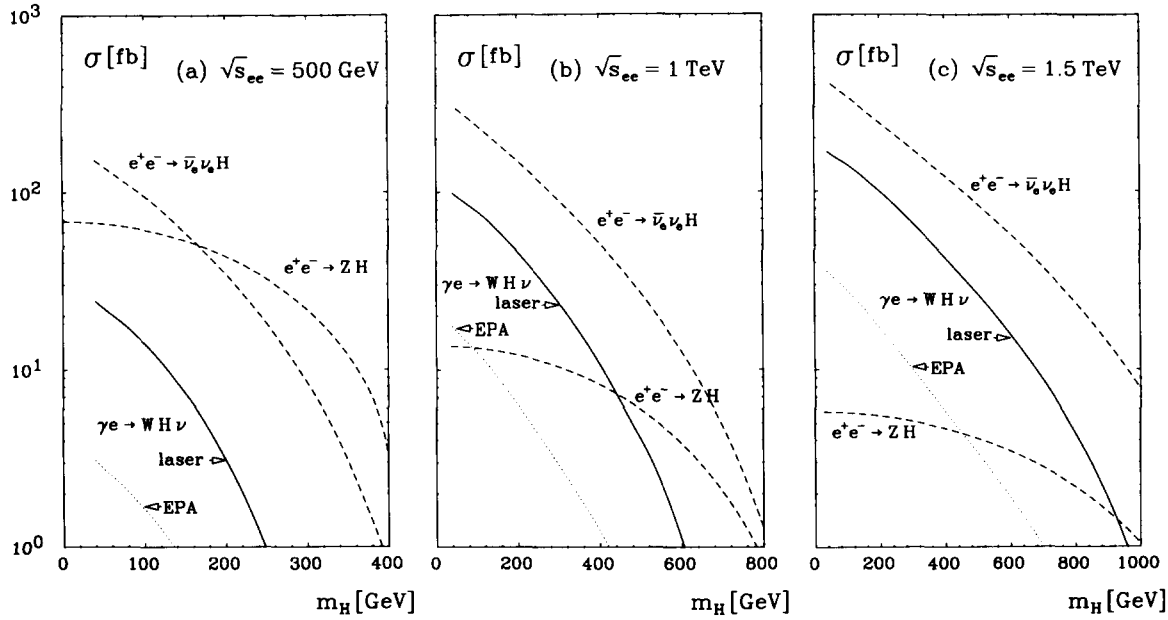

Fig. 4. Comparison of the photon cross section for Higgs production in Compton back-scattering, $\gamma+e^-\to W^-+H+\nu_e$ (solid lines), with the standard bremsstrahlung process $e^+e^-\to Z+H$ and the fusion process $e^+e^-\to\bar{\nu}_e\nu_e+H$ (dashed lines). The evWH production cross sections for the Weizsäcker–Williams photon spectra are shown by the dotted lines. The energies are the e^+e^- collider CM energies (a) 500 GeV, (b) 1 TeV and (c) 1.5 TeV.

laser and dotted lines for Weizsäcker–Williams photons), together with the standard Higgs production cross sections $e^+e^-\to ZH$ and $e^+e^-\to\bar{\nu}\nu H$ (dashed lines), at three typical e^+e^- collision energies (a) 500 GeV, (b) 1 TeV and (c) 1.5 TeV. While the standard cross sections are clearly dominating at moderate e^+e^- energies, the laser induced $e\gamma$ cross section rises to a size similar to the dominant fusion cross section at high energies. It should be noted that the cross section for evWH photoproduction dominates over the ZH cross section for moderate m_H values, even for the case of automatically generated Weizsäcker–Williams photons.

The process (1) can be approximated well at high energies by the subprocess $\gamma W\to WH$, where the initial W is the equivalent real W boson inside the $e^\pm$ beams [8]. The cross section for the production of Higgs particles on W targets, $\gamma W\to WH$, can easily be calculated by evaluating the associated subdiagrams in fig. 1. The maximal physical information is summarized in the helicity amplitudes which we present in the γW CM frame. Denoting the initial and final state helicities of the W's by λ_i and λ_f, respectively, and the γ helicity by λ_γ, the helicity amplitudes may be written as

$$\mathcal{M}^{\lambda_f\lambda_i}_{\lambda_\gamma}=-egm_W\sqrt{s}\left[\left(\frac{1}{s-m_W^2}+\frac{1}{t-m_W^2}\right)\mathcal{A}^{\lambda_f\lambda_i}_{\lambda_\gamma}+\frac{1}{t-m_W^2}\mathcal{B}^{\lambda_f\lambda_i}_{\lambda_\gamma}\right], \tag{7}$$

s is the square of the CM energy, t the four-momentum transfer squared from the photon to the final state W-boson. The associated scattering angle is ϑ. By introducing the scaling variables β and $\bar{\beta}$ of the initial and final W's in the γW CM frame,

$$\beta_i=2p_i^*/\sqrt{s},\quad \beta_f=2p_f^*/\sqrt{s},\quad \bar{\beta}_i=2E_i^*/\sqrt{s},\quad \bar{\beta}_f=2E_f^*/\sqrt{s}, \tag{8}$$

the reduced amplitudes $\mathcal{A}$ and $\mathcal{B}$ can be expressed as

$$\mathscr{A}^{\lambda_f\lambda_i}_{\lambda_\gamma} = \frac{1+\lambda_i\lambda_\gamma}{2}\lambda_f\beta_i\frac{\sin\vartheta}{\sqrt{2}}, \qquad \text{for } \lambda_f, \lambda_i = \pm 1,$$

$$= \frac{\sqrt{s}}{m_W}\beta_i\frac{1+\lambda_f\lambda_\gamma\cos\vartheta}{2}, \qquad \lambda_f = \pm 1, \lambda_i = 0,$$

$$= -\frac{\sqrt{s}}{m_W}\beta_i\frac{1+\lambda_i\lambda_\gamma}{2}\frac{\beta_f-\bar{\beta}_f\cos\vartheta}{2}, \qquad \lambda_f = 0, \lambda_i = \pm 1,$$

$$= -\frac{s}{2m_W^2}\lambda_\gamma\bar{\beta}_f\beta_i\frac{\sin\vartheta}{\sqrt{2}}, \qquad \lambda_f = \lambda_i = 0 \tag{9}$$

and

$$\mathscr{B}^{\lambda_f\lambda_i}_{\lambda_\gamma} = \lambda_\gamma\beta_f\frac{1-\lambda_f\lambda_i\cos\vartheta}{2}\frac{\sin\vartheta}{\sqrt{2}}, \qquad \text{for } \lambda_f, \lambda_i = \pm 1,$$

$$= \frac{\sqrt{s}}{m_W}\frac{\lambda_f\lambda_\gamma}{2}\beta_f\bar{\beta}_i\frac{\sin^2\vartheta}{2}, \qquad \lambda_f = \pm 1, \lambda_i = 0,$$

$$= \frac{\sqrt{s}}{m_W}\frac{\lambda_i\lambda_\gamma}{2}\beta_f\bar{\beta}_f\frac{\sin^2\vartheta}{2}, \qquad \lambda_f = 0, \lambda_i = \pm 1,$$

$$= \frac{s}{2m_W^2}\lambda_\gamma\beta_f\frac{\beta_f\beta_i+\bar{\beta}_f\bar{\beta}_i\cos\vartheta}{2}\frac{\sin\vartheta}{\sqrt{2}}, \qquad \lambda_f = \lambda_i = 0. \tag{10}$$

Although the amplitudes for $\lambda_f=\lambda_i=0$ ($\gamma W_L \to W_L H$) may superficially seem to violate the unitarity constraint at high energies, we find that at asymptotic energies they reduce to

$$\mathscr{M}^{00}_{\pm} = \pm eg\frac{m_H^2}{2m_W\sqrt{s}}\left(1-\frac{m_H^2}{s}\right)\frac{s}{t-m_W^2}\frac{\sin\vartheta}{\sqrt{2}}\left[1+O\left(\frac{m_W^2}{s}\right)\right]. \tag{11}$$

This amplitude agrees up to terms of $O(m_W)$ with the associated Goldstone boson scattering amplitudes, in accordance with the equivalence theorem [9]. In addition, the following helicity amplitudes contribute to the asymptotic cross section:

$$\mathscr{M}^{\pm 0}_{\pm} = -eg\frac{s}{t-m_W^2}\frac{1+\cos\vartheta}{2}+O\left(\frac{m_W^2}{s}\right). \tag{12}$$

After integration over the scattering angle of the squared amplitudes, only the above amplitudes with an initial W_L ($\lambda_i=0$) give asymptotically non-vanishing total cross sections.

$$\sigma(\gamma W\to WH) = \frac{e^2g^2}{16\pi m_W^2}\left(1-\frac{m_H^2}{s}\right)\left[1+\frac{m_H^4}{2s^2}\left(\ln\frac{(s-m_H^2)^2}{sm_W^2}-2\right)+O\left(\frac{m_W^2}{s}\right)\right]. \tag{13}$$

This asymptotic cross section is built-up by the fusion of the initial W_L radiated from the electron or positron, and the quasi-real W_L inside the photon the distribution of which is given by

$$D_{W_L/\gamma}(x) = \frac{\alpha}{\pi}\left[\frac{1-x}{x}+\frac{x(1-x)}{2}\left(\ln\frac{s(1-x)^2}{m_W^2}-2\right)\right]. \tag{14}$$

The equivalent W_L distribution inside the photon is similar in magnitude at small energy fraction x to the well-known W_L distribution inside the electron [8]:

$$D_{W_{L/e}}(x)=\frac{\alpha}{4\pi \sin^2\theta_w}\frac{1-x}{x}, \tag{15}$$

but is more abundant at large x due to the hard component with the logarithmic enhancement factor. The relatively large magnitude of the $\gamma e \to WH\nu$ production cross section up to high values of m_H at $\sqrt{s}=1.5$ TeV (fig. 4c) can be interpreted as a manifestation of the hard effective real W_L distribution inside the photon. At multi-TeV energies, laser induced γ beams become almost as efficient sources of energetic W_L's as the original $e^{\pm}$ beams.

We thank M. Drees, H. Murayama and F. Schrempp for valuable discussions. One of us (K.H.) wishes to thank the UK Science and Engineering Research Council for a Visiting Fellowship. K.H. and P.Z. gratefully acknowledge the hospitality extended to them by A. Martin during their visits to Durham University where this study was initiated.

Note added. While finalizing this letter, we learned about a parallel study by Boos et al. [10] with similar conclusions.

References

[1] K. Hagiwara, H. Iwasaki, A. Miyamoto, H. Murayama and D. Zeppenfeld, Nucl. Phys. B 365 (1991) 544, and references therein.
[2] I.F. Ginzburg, G.L. Kotkin, V.G. Serbo and V.I. Telnov, Nucl. Instrum. Methods 205 (1983) 47;
I.F. Ginzburg, G.L. Kotkin, S.L. Panfil, V.G. Serbo and V.I. Telnov, Nucl. Instrum. Methods 219 (1984) 5.
[3] K. Hagiwara, I. Watanabe and H. Murayama, preprint KEK-TH-264 (1990), Nucl. Phys. B (1991), to be published.
[4] H. Murayama, I. Watanabe and K. Hagiwara, HELAS, HELicity Amplitude Subroutines for Feynman diagrams, KEK Report, to be published.
[5] T.L. Barklow, in: Proc. (Snowmass, CO, 1990), and SLAC-PUB-5364 (1990).
[6] E. Yehudai, Ph.D. Thesis, SLAC Report SLAC-383 (1991).
[7] S.Y. Choi and F. Schrempp, DESY preprint 91-068.
[8] S. Dawson, Nucl. Phys. B 249 (1984) 42;
G.L. Kane, W.W. Repko and W.B. Rolnick, Phys. Lett. B 148 (1984) 367.
[9] B.W. Lee, C. Quigg and H.B. Thacker, Phys. Rev. D 16 (1977) 1519;
M.S. Chanowitz and M.K. Gaillard, Nucl. Phys. B 261 (1985) 379.
[10] E. Boos et al., DESY preprint 91-114.